

# A BLIND TRANSFORM BASED APPROACH FOR THE DETECTION OF ISOLATED ASTROPHYSICAL PULSES

*Marwan Alkhweldi, Natalia A. Schmid*

LDCSEE, West Virginia University  
Morgantown, WV 26506, USA

*Richard M. Prestage*

National Radio Astronomy Observatory  
Route 28/92, Green Bank, WV 24944, USA

## ABSTRACT

This paper presents a blind algorithm for the automatic detection of isolated astrophysical pulses. The detection algorithm is applied to spectrograms (also known as “filter bank data” or “the (t,f) plane”). The detection algorithm comprises a sequence of three steps: (1) a Radon transform is applied to the spectrogram, (2) a Fourier transform is applied to each projection parametrized by an angle, and the total power in each projection is calculated, and (3) the total power of all projections above  $90^\circ$  is compared to the total power of all projections below  $90^\circ$  and a decision in favor of an astrophysical pulse present or absent is made. Once a pulse is detected, its Dispersion Measure (DM) is estimated by fitting an analytically developed expression for a transformed spectrogram containing a pulse, with varying value of DM, to the actual data. The performance of the proposed algorithm is numerically analyzed.

**Index Terms**— Fast Radio Bursts (FRB), astrophysical pulse, blind detection, dispersion measure, estimation, filter bank data, Radon transform.

## 1. INTRODUCTION

Fast Radio Bursts (FRB) are short-duration isolated radio bursts of extragalactic nature [1, 2]. The origin of these mysterious sources is currently unclear. Some possible sources that have so far been proposed to explain FRBs include collapsing neutron stars [3], coalescing neutron-star binaries [4], evaporating black holes [5], or cosmic strings [6]. Efficiently finding more bursts will unlock their cause and may enable the use of FRBs to probe the universe.

From a signal processing perspective, detecting single isolated astronomical pulses is a challenging task. When a telescope such as the Green Bank Telescope [7] is used to survey the sky, gigabytes of radio astronomical data are streamed and stored on disks in a matter of minutes. Therefore searching for the astrophysical pulses in real time would save not only the processing time but also the storage space.

Radio astronomical telescopes are designed to receive a broad band signal, typically of order of hundreds of MHz. The main distinctive feature of an astrophysical pulse is its

dispersed nature - the lower frequency components of the pulse are delayed compared to higher frequency components. The time delay is proportional to the density of free electrons in the interstellar medium integrated over the distance that the pulse travels. A well-established conventional approach to the astrophysical pulse detection compensates for the delay in low frequencies first and then integrates the signal over the entire frequency range [8]. This process, known as de-dispersion, boosts the SNR of the pulse signal. The conventional de-dispersion followed by a matched filter detection approach involves an exhaustive search for the correct dispersion measure (DM) over a broad range of possible values. Nearly all FRBs discovered in the past were detected using the conventional approach and its variants [9, 10] with the exclusion of a few most recently discovered FRBs, where new, fast detection algorithms based on transform methods [11, 12, 13] have been involved.

This work is inspired by an approach described by Weber et al [14], which suggested the application of a two-dimensional Fourier transform followed by a Hough transform as a means of detecting giant pulses emitted by neutron stars. We propose a new alternative blind approach for the detection of isolated astrophysical pulses. The approach exploits the efficiency of two transform methods, the Radon transform and the Fourier transform. A Radon transform is applied to a broad band spectrogram – the astrophysical signal stored as a two-dimensional function of time and frequency (also known in radio astronomy as filter bank data). The output of the Radon transform is presented as a set of projections parametrized by an angle parameter. The Fourier transform is applied to each projection, and the total power in each projection is evaluated. The detection algorithm compares the total power in all projections to the left and right of  $90^\circ$ . Once an astrophysical pulse is detected, its DM value is estimated by means of a least square approach involving an analytical signature derived in this work. The performance of the developed blind detection algorithm and the performance of the DM estimation approach are demonstrated on simulated data.

The remainder of the paper is organized as follows. Sec. 2 provides details of the proposed detection algorithm. Sec.

3 describes a least square approach for estimation of the DM value. Sec. 4 presents the results of a performance analysis. A short summary is presented in Sec. 5.

## 2. DETECTION ALGORITHM

The detection algorithm comprises three main steps. A block-diagram illustrating them is shown in Fig.1. A detailed de-

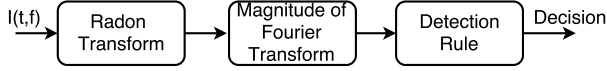


**Fig. 1.** A block diagram of the proposed detection approach.

scription of each block in the block-diagram is provided below.

### 2.1. Radon transform

The first block in Fig.1 applies the Radon transform to filter bank data. Denote by  $I(t, f)$  the filter bank data (treated here as an image), then the Radon transform is mathematically defined as [15]

$$R_{\theta}(\rho) = \int_{t_i}^{t_f} \int_{f_l}^{f_h} I(t, f) \delta(\rho - t \cos \theta - f \sin \theta) dt df, \quad (1)$$

where  $\theta$  is the angle of a projection,  $\rho$  is the offset of a projection line from the origin of the  $(t, f)$  plane,  $t_i, t_f, f_l$  and  $f_h$  define four time-frequency boundary points of the  $(t, f)$  plane and  $\delta(\cdot)$  is the Dirac delta function. Assuming that an astrophysical pulse has a Gaussian profile,  $I(t, f)$  can be expressed as

$$I(t, f) = h \exp\left(-\frac{t^2}{2c^2}\right) \delta(f) \quad (2)$$

$$** \delta\left(t_{ref} - t - 4.15 \times 10^3 \times \text{DM} \left(f_{ref}^{-2} - f^{-2}\right)\right),$$

where  $h$  is the peak of the pulse profile in a frequency channel, the parameter  $c$  is related to the full width at half maximum (FWHM) according to  $\text{FWHM} = 2\sqrt{2 \ln 2} c$ ,  $t_{ref}$  is the reference time,  $f$  is the radio frequency of a channel, measured in MHz,  $f_{ref}$  is a reference frequency in MHz (related to  $t_{ref}$ ), DM stands for the dispersion measure in the units of  $\text{pc}/\text{cm}^3$ , and  $**$  stands for a two-dimensional convolution.

Fig.2 provides an example of applying the Radon transform to the ‘‘Lorimer burst’’ – the first FRB to be discovered [1] – at a specific angle  $\theta = 76^\circ$ . Fig.3(c) shows the Radon transform of the Lorimer burst in panel (a). Fig.3(d) displays the Radon transform of the filter bank data shown in panel (b), which presents noise plus radio frequency interference (RFI) – unwanted terrestrial signals – but no astrophysical pulse.

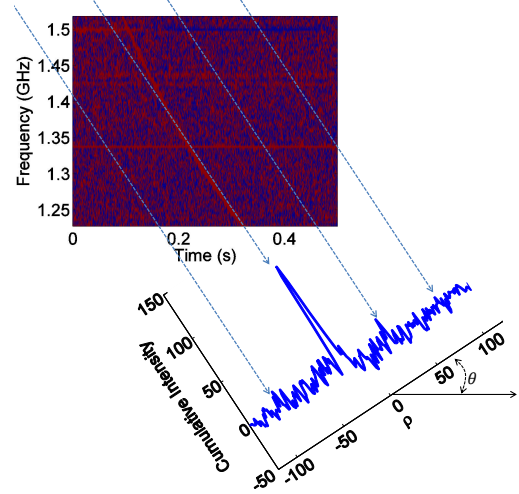


**Fig. 2.** The result of applying the Radon transform to the Lorimer burst at the orientation  $\theta = 76^\circ$ .

### 2.2. Fourier transform

As a second step, the algorithm applies the one dimensional Fourier transform along the columns of Radon transformed filter bank data. The Fourier transform for a projection of an image at angle  $\theta$  can be found as

$$r_{\theta}(u) = \int_{-\infty}^{\infty} R_{\theta}(\rho) \exp(-j2\pi u \rho) d\rho, \quad (3)$$

where  $u$  represents a frequency. Fig.2 shows an example of projecting the Lorimer burst at an angle  $\theta = 76^\circ$ , where Fig.4 shows the magnitude of the Fourier transform of the projection. Figs.3(e,f) show the magnitude of the Fourier transform of Fig.3(c,d), respectively. The sum of magnitudes of the data in panels (e) and (f) is shown in panels (g) and (h). The sum is performed along the columns.

In Fig.3(g), the signature of the Lorimer burst appears as a relatively strong and approximately Gaussian shaped pulse in the range of projection angles  $\theta \in [71^\circ, 79^\circ]$ . A large spike at  $\theta = 90^\circ$  is due to the existence of RFI in the data. RFI is characterized by a zero DM value and may be broadband at a single time (bursty) or persistent at a single frequency. Such interference shows up at  $\theta = 0^\circ$  and  $\theta = 90^\circ$  in the magnitude of the Fourier transform. RFI has intentionally been left in the figures presented here, to illustrate its effect. This is normally removed by our algorithm by simply suppressing the power in the projections around  $0^\circ$  and  $90^\circ$ . (The conventional pulse detection approach also removes RFI prior to the pulse detection process.)

### 2.3. Decision rule

The pulse can be detected by evaluating the overall power in the projections. As observed from the panels (g) and (h) in Fig. 3, the power distribution is nearly symmetric around

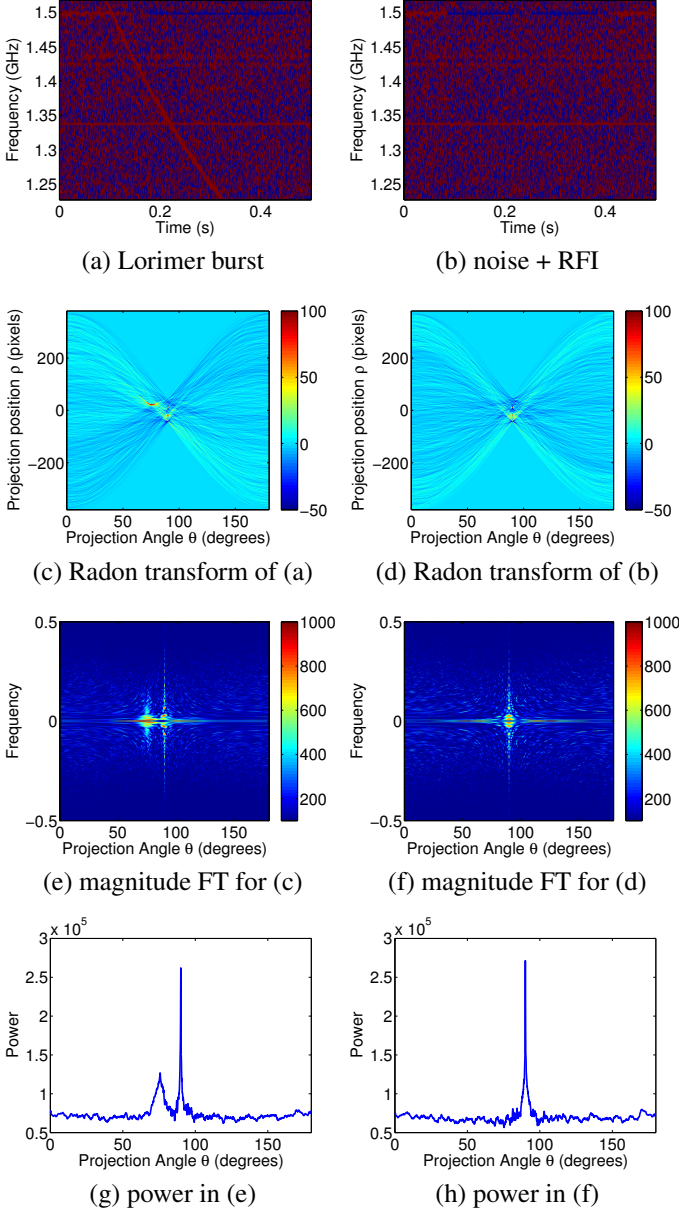


**Fig. 3.** Filter bank data in (a) and (b) and their stepwise transformations.

$90^\circ$  for the case when no pulse (noise only case) is present in the data. As was noted earlier, for the case when the data contain a pulse, the power distribution is skewed due to the dispersion relationship in Eqn. 2.

Denote by  $r_\theta$  the cumulative power in the projection at an angle  $\theta$ . Then comparing the total power in the projections below and above  $90^\circ$  leads to the following intuitive decision rule. Decide a pulse is present if

$$\sum_{\theta=\epsilon}^{90^\circ-\epsilon} |r_\theta|^2 > \gamma \sum_{\theta=90^\circ+\epsilon}^{180^\circ-\epsilon} |r_\theta|^2, \quad (4)$$

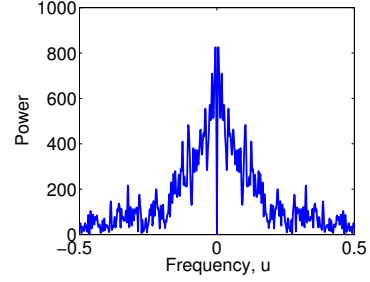


**Fig. 4.** The magnitude of the Fourier transform of the projection of the Lorimer Burst at  $\theta = 76^\circ$ .

where  $\epsilon$  is a small number introduced to avoid inclusion of RFI and  $\gamma$  is a decision threshold ( $\gamma > 1$ ). The pulse is not detected, otherwise.

### 3. ESTIMATION OF DM VALUE

Once the pulse is detected, we have enough information to estimate its DM value. A basic approach to the estimation problem is to establish upper and lower bounds on the DM value via a linearization of the dispersion equation. This solution is used as a baseline in performance evaluation.

Fitting an analytically derived signature of an astronomical pulse into the Fourier transform of projection lines is an alternative least square solution to the same problem. We outline the second solution below.

After combining Eqns. 2 and 3 we obtain

$$r_\theta(u) = \int_{t_i}^{t_f} \int_{f_l}^{f_h} I(t, f) \times \int_{-\infty}^{\infty} \delta(\rho - t \cos \theta - f \sin \theta) e^{-j2\pi\rho u} d\rho dt df. \quad (5)$$

Integrating out  $\rho$  results in

$$r_\theta(u) = \int_{t_i}^{t_f} \int_{f_l}^{f_h} I(t, f) e^{-j2\pi(t \cos \theta + f \sin \theta)u} dt df, \quad (6)$$

which is a two-dimensional Fourier transform with spatial frequencies replaced by  $u \cos \theta$  and  $u \sin \theta$ . From Eqn. 2 and the convolution property of the Fourier transform, Eqn. 6 becomes

$$r_\theta(u) = \int_{f_l}^{f_h} e^{-j2\pi(u \cos \theta \frac{d}{f^2} + u \sin \theta)} df \times e^{-j2\pi u \left( t_{ref} - \frac{d}{f_{ref}^2} \right)} \sqrt{2\pi h} e^{-\frac{c^2}{2} (2\pi)^2 (u \cos \theta)^2}. \quad (7)$$

Then the least square solution to the estimation problem is given as

$$\widehat{DM} = \arg \min_{DM \in [DM_{min}, DM_{max}]} \|x_\theta(u) - r_\theta(u)\|^2, \quad (8)$$

where the distance is evaluated over all values  $\theta$  and  $u$  such that the estimated signal power in the data  $|x_\theta(u)|^2$  exceeds the estimated noise variance  $\sigma^2$  in the data.

#### 4. PERFORMANCE ANALYSIS

In this section the performance of the detection and DM estimation algorithms is evaluated. The performance of the detection algorithm is demonstrated through Receiver Operating Characteristic (ROC) curves [16]. Due to a very limited amount of practical data containing real FRB pulses (only 20 FRBs are known thus far), our numerical evaluation is based on simulated data. The initial data are displayed in filter bank format, where astrophysical pulses are dispersed according to Eqn. 2. We assume that the pulse profile is Gaussian with the FWHM set to 4.6 ms. The bandwidth of the simulated filter bank data is set to 288 MHz, the center frequency  $f_c$  is equal to 1374 MHz. The bandwidth is partitioned into  $K = 96$  discrete frequency channels, and the time resolution is set to 0.25 ms. To add the noise to the simulated astrophysical pulse, we apply the conventional definition of the signal-to-noise ratio, where it is defined as a ratio of the peak value of a de-dispersed and matched-filtered observed signal, to the root mean square (RMS) of the simulated noise. For a fixed value

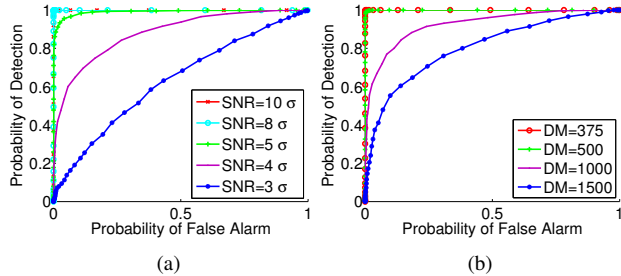


**Fig. 5.** ROC curve (a) as a function of signal to noise ratio (DM=375pc/cm<sup>3</sup>) (b) as a function of DM (SNR=10σ).

of DM we vary the value of SNR from 10σ down to 3σ, where σ is the estimated RMS value of the noise in the de-dispersed filter bank data. The results of the performance evaluation parameterized by the DM value 375pc/cm<sup>3</sup> are displayed in Fig. 5(a). Each ROC curve shown in the figure is generated using 1000 Monte Carlo realizations of filter bank data including noisy realizations of simulated astronomical pulses and also noise only realizations. The results in Fig.5(a) indicate that at SNR level 5σ and higher the probability of miss is very low while the probability of detecting the true astrophysical pulses is relatively high (for example, the detection rate is 0.95 at a cost of false alarm rate equal to 0.05).

Fig. 5(b) demonstrates how the detection rate improves with decreasing the value of DM. Note that in this case the SNR value is set to 10σ.

The results of the analysis of the DM estimation problem are presented in Fig. 6. We demonstrate the results of the

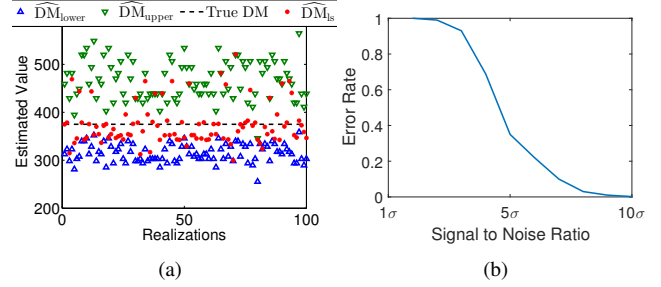


**Fig. 6.** Interval estimate of DM (a) 100 realizations (SNR = 10σ) (b) estimation error rate as a function of SNR.

DM estimation due to the approach outlined by Eqn. 8. We also plot the upper and lower bounds on the DM value of a simulated astrophysical pulse. The results are displayed for the case of the SNR value set to 10σ.

Fig. 6(a) demonstrates that the true value of DM is within the interval between  $\widehat{DM}_{lower}$  and  $\widehat{DM}_{upper}$ . Due to the fact that estimator function in Eqn. 8 is nonlinear function in  $\theta$ , the  $\widehat{DM}_{upper}$  values are more spread compared to  $\widehat{DM}_{lower}$ . Fig. 6(b) displays the probability of error as a function of SNR. The probability of estimation error is referred to the percentage of times a true DM value is falling outside of the estimated lower and upper bounds.

#### 5. SUMMARY

This paper introduced a blind (fully automated) detection algorithm for the detection of isolated astrophysical pulses. The algorithm involves two transformations, the Radon transform followed by the Fourier transform, and comprises three main steps. Compared to the conventional detection algorithm used in radio astronomy for the detection of isolated pulses, the proposed detection algorithm does not require any searching for the value of the unknown DM, which is computationally expensive.

The performance of the detection algorithm is displayed as a set of ROC curves. Two parameters are varied, the SNR value and the DM value. The ROC curves show that a good detection performance can be achieved at the SNR level 5σ and above, which is a typical choice of the threshold for the conventional detection algorithm.

Once an astrophysical pulse is detected, we apply a least squares approach to estimate the DM value of the pulse. The performance of the DM estimation algorithm is analyzed in terms of the probability of estimation error. Through Monte Carlo simulations we have demonstrated that the estimated DM values are in the average 50pc/cm<sup>3</sup> apart from the true DM value (with 150pc/cm<sup>3</sup> being the maximal deviation).

## 6. REFERENCES

- [1] D. R. Lorimer, M. Bailes, M. A. McLaughlin, D. J. Narkevic, and F. Crawford, "A bright millisecond radio burst of extragalactic origin," *Science*, vol. 318, pp. 777–780, Nov. 2007.
- [2] D. Thornton, B. Stappers, M. Bailes, B. Barsdell, S. Bates, N. D. R. Bhat, M. Burgay, S. Burke-Spolaor, D. J. Champion, P. Coster, N. D'Amico, A. Jameson, S. Johnston, M. Keith, M. Kramer, L. Levin, S. Milia, C. Ng, A. Possenti, and W. van Straten, "A population of fast radio bursts at cosmological distances," *Science*, vol. 341, pp. 53–56, July 2013.
- [3] H. Falcke and L. Rezzolla, "Fast radio bursts: the last sign of supramassive neutron stars," *Astronomy & Astrophysics*, vol. 562, p. 137, 2014.
- [4] T. Totani, "Cosmological Fast Radio Bursts from Binary Neutron Star Mergers," *PASJ*, vol. 65, p. 12, 2014.
- [5] M. J. Rees, "A better way of searching for black-hole explosions," *Nature*, vol. 266, p. 333, Mar. 1977.
- [6] Y.-F. Cai, E. Sabancilar, D. A. Steer, and T. Vachaspati, "Radio broadcasts from superconducting strings," *Phys. Rev. D.*, vol. 86, p. 043521, Aug. 2012.
- [7] R. M. Prestage, K. T. Constantinescu, T. R. Hunter, L. J. King, R. J. Lacasse, F. J. Lockman, and R. D. Norrod, "The Green Bank Telescope," *IEEE Proceedings*, vol. 97, pp. 1382–1390, Aug. 2009.
- [8] S. Ransom, "Pulsar exploration and search toolkit, presto." <http://www.cv.nrao.edu/~sransom/presto/>.
- [9] B. R. Barsdell, M. Bailes, D. G. Barnes, and C. J. Fluke, "Accelerating incoherent dedispersion," *Monthly Notices of the Royal Astronomical Society*, vol. 422, p. 379392, 2012.
- [10] N. Clarke, J. P. Macquart, and C. Trott, "Performance of a novel fast transient detection system," *The Astrophysical Journal Supplement Series*, vol. 205, p. 4, Feb. 2013.
- [11] B. Zackay and E. O. Ofek, "An accurate and efficient algorithm for detection of radio bursts with an unknown dispersion measure, for single dish telescopes and interferometers," *The Astrophysical Journal*, 2014.
- [12] L. G. Spitler, J. M. Cordes, J. W. T. Hessels, D. R. Lorimer, M. A. McLaughlin, S. Chatterjee, F. Crawford, J. S. Deneva, V. M. Kaspi, R. S. Wharton, B. Allen, S. Bogdanov, A. Brazier, F. Camilo, P. C. C. Freire, F. A. Jenet, K.-A. C., B. Knispel, P. Lazarus, K. J. Lee, J. van Leeuwen, R. Lynch, S. M. Ransom, P. Scholz, X. Siemens, I. H. Stairs, K. Stovall, J. K. Swiggum, A. Venkataraman, W. W. Zhu, C. Aulbert, and H. Fehrmann, "Fast radio burst discovered in the arecibo pulsar alfa survey," *The Astrophysical Journal*, vol. 790, p. 101, Jul. 2014.
- [13] K. Masui, H.-H. Lin, J. Sievers, C. J. Anderson, T.-C. Chang, X. Chen, A. Ganguly, M. Jarvis, C.-Y. Kuo, Y.-C. Li, *et al.*, "Dense magnetized plasma associated with a fast radio burst," *Nature*, vol. 528, no. 7583, pp. 523–525, 2015.
- [14] D. Ait-Allal, R. Weber, C. Dumez-Viou, I. Cognard, and G. Theureau, "Blind detection of giant pulses: Gpu implementation," *Comptes Rendus Physique*, vol. 13, no. 1, pp. 80–87, 2012.
- [15] S. Deans, *The radon transform and some of its applications*. New York: John Wiley and Sons, 1983.
- [16] H. Van Trees, *Detection, Estimation, and Modulation Theory, Part I*. John Wiley and Sons, 2001.